

Drying cellulose nanofibrils: in search of a suitable method

Yucheng Peng · Douglas J. Gardner · Yousoo Han

Received: 13 September 2011 / Accepted: 24 November 2011
© Springer Science+Business Media B.V. 2011

Abstract Increasing research activity on cellulose nanofibril-based materials provides great opportunities for novel, scalable manufacturing approaches. Cellulose nanofibrils (CNFs) are typically processed as aqueous suspensions because of their hydrophilic nature. One of the major manufacturing challenges is to obtain dry CNFs while maintaining their nano-scale dimensions. Four methods were examined to dry cellulose nanocrystal and nanofibrillated cellulose suspensions: (1) oven drying, (2) freeze drying (FD), (3) supercritical drying (SCD), and (4) spray-drying (SD). The particle size and morphology of the CNFs were determined via dynamic light scattering, transmission electron microscopy, scanning electron microscopy, and morphological analysis. SCD preserved the nano-scale dimensions of the cellulose nanofibrils. FD formed ribbon-like structures of the CNFs with nano-scale thicknesses. Width and length were observed in tens to hundreds of microns. SD formed particles with a size distribution ranging from nanometer to several microns. Spray-drying is

proposed as a technically suitable manufacturing process to dry CNF suspensions.

Keywords Cellulose nanofibril · Drying · Freeze drying · Supercritical drying · Spray-drying

Introduction

The study of cellulose nanofibrils (CNFs) and their application as a reinforcing component in polymer composites has received considerable attention (Beecher 2007; Hubbe et al. 2008; Siro and Plackett 2010; Habibi et al. 2010; Eichhorn et al. 2010; Siqueira et al. 2010; Klemm et al. 2011; Moon et al. 2011). With the size decrease from bulk wood cells to nanofibrils, the elastic modulus of cellulose increases from about 10 to 70 GPa (Jeronimidis 1980) or higher (145 GPa) (Beecher 2007), which results in significant mechanical property improvement for cellulose nanofibril-reinforced polymer composites. The biodegradability, low density, worldwide availability, low price and modifiable surface properties of these novel materials provide potential opportunities to develop a new generation of materials based on cellulosic fibers. These CNFs can be used as a replacement for conventional reinforcements such as glass fibers or inorganic fillers in composites but are not widely commercially available, although recent reports indicate pilot-scale quantities will soon be available in Canada, Europe, and the US (O'Connor 2011;

Y. Peng · D. J. Gardner (✉) · Y. Han
AEWC Advanced Structures and Composites Center,
University of Maine, 5793 AEWB Building, Orono,
ME 04469, USA
e-mail: douglasg@maine.edu

Y. Peng · D. J. Gardner · Y. Han
School of Forest Resources, University of Maine,
5793 AEWB Building, Orono, ME 04469, USA

Vartiaine et al. 2011; Bloch 2011). In most cases, CNFs are processed as aqueous suspensions because of their hydrophilic nature and propensity to agglomerate during drying (Gardner et al. 2008). There is a well perceived need to develop robust processes to dry CNF which will maintain nano-scale dimensions for materials applications where a dry form is necessary and, secondarily, to mitigate the higher transportation costs of the aqueous suspensions. Having a dried form of CNF is especially important in the field of thermoplastic processing like extrusion or injection molding where thermal melting processes are encountered. During thermal melting processes with non-polar thermoplastics, water is a detriment to satisfactory processing. Therefore, drying of aqueous suspensions of CNFs and understanding the drying process are necessary for their utilization in developing industrially relevant polymer nanocomposites.

Four different forms of cellulose fibrils on the nano-scale can be prepared (Gardner et al. 2008). Two of them were studied in this research work. With wood pulp as the raw material, CNFs are manufactured by two general methods: mechanical fibrillation and chemical hydrolysis. The corresponding products are referred to as nanofibrillated cellulose (NFC) and cellulose nanocrystals (CNC), respectively. NFC is obtained by processing dilute slurries of cellulose fibers through grinding or high-pressure homogenizing action while the production of cellulose nanocrystals involves the digestion of amorphous cellulosic domains by an acid hydrolysis process (Herrick et al. 1983; Hubbe et al. 2008). After manufacturing, an evenly dispersed CNF aqueous suspension occurs as a colloidal system. The strong hydrogen bonds among water and cellulose particles enable the system to remain thermally or kinetically stable throughout a range of water contents. Water can penetrate into amorphous regions of NFC while it can only hydrogen bond to the surfaces of CNCs or to the crystalline regions of NFCs. The adsorbed water on cellulose fibers is categorized into three different states based on the thermodynamic property of water: free water, freezing bound water, and nonfreezing bound water (Nakamura et al. 1981). Free water is defined as bulk water with the same thermal characteristics of pure water. Freezing bound water is water reacted with hydroxyl groups on cellulose molecules; the transition temperature is lower than pure water because of the restriction of reactions between water and cellulose

fibers. Nonfreezing bound water is defined as a subset of bound water with a non-detectable thermal transition. At the same time, nonfreezing bound water is interpreted as water reacting with hydroxyl groups of cellulose molecules directly while freezing bound water is located relatively far away from the hydroxyl groups (Weise et al. 1996). Some of the freezing bound water molecules might not be bound to the hydroxyl groups, but are still close enough to be influenced by these hydrophilic groups and exhibit a depressed transition temperature.

Removing water from CNF suspensions to maintain nano-scale dimensions of the nanofibrils is a delicate process. Dehydration of CNF suspensions using ethanol showed significant increase in nanofibril diameter (Thimm et al. 2000). The existence of air–water interfaces with fibril-sized curvature in the suspensions may exert sufficient attractive capillary pressures to displace fibrils from their original positions. These capillary forces have been demonstrated by pulling adjacent fibers together in the wet state of paper (Lyne and Galay 1954). At the same time, mutual diffusion of nano-scale fibrils at interfacing surfaces may also drive the CNFs to agglomerate. The molecular segments of cellulose fibrils which are partially dissolved in water (Clark 1985) tend to mix in the wet state, resulting in interpenetration and tangling among the nano-scale cellulose fibrils (McKenzie 1984; Pelton 1993). In addition, hydrogen bonds and Van der Waals forces are expected to hold the fibrils together after the removal of water (Hiemenz and Rajagopalan 1997; Hunter 2001). Hydrogen bonding among CNFs requires that hydroxyl groups at the facing surfaces approach each other within 0.25–0.35 nm, i.e. molecular contact. For dispersion forces (Van der Waals) to occur, the distances among nanofibrils need to be closer than the distances for hydrogen bonds (Hiemenz and Rajagopalan 1997; Lindstrom et al. 2005). In a stable CNF suspension, the distances among fibrils are not small enough to form molecular contact. During drying, forces resulting from the removal of water and high temperatures may drive the molecular contact of CNFs and cause agglomeration. The objective of our study is to identify a suitable drying process to produce reasonable quantities of dry cellulose nanofibrils. Three methods are proposed to dry the CNFs: freeze drying, spray-drying, and supercritical drying (Pakowski 2007). Oven drying of CNF suspensions will be performed as a control.

Experimental

Suspension preparation

Two CNF suspensions were involved: (1) a commercial product of NFC suspension ARBOCEL MF40–10 at 10 wt. % from J. Rettenmaier & Sohne GMBH+CO.KG, Germany, and (2) a CNC suspension at 6.5 wt. % from the Forest Products Laboratory in Madison, Wisconsin. Before drying, distilled water was added into the original suspensions and mixed using a Speed Mixer[®] (Flack Tek Inc., US) for 4 min at 2,000 rpm to obtain final weight concentrations of CNC and NFC suspensions at 0.001, 0.1, and 2%.

Dynamic light scattering (DLS)

Measurements of all cellulose nanofibril suspensions at 0.1 wt. % were made with a Zetasizer Nano ZS (Malvern Instruments, Malvern UK) using a detection angle of 173° at a temperature of 25 °C. The viscosity value for water was used in all measurements. The Nano ZS uses a 4mW He–Ne laser operating at a wavelength of 633 nm. The intensity size distributions were obtained from analysis of the correlation functions using the Multiple Narrow Modes algorithm in the instrument software. This algorithm is based upon a non-negative least squares fit (Lawson and Hanson 1995; Desobry et al. 1997). These intensity particle size distributions were converted into volume using Mie theory (Mie 1908).

Transmission electron microscopy (TEM)

Drops of 0.001 wt. % NFC and CNC suspensions were deposited on carbon coated electron microscope grids and negatively stained with 2 wt. % uranyl acetate. The grids were dried in air and observed with a Philips CM10 Transmission Electron Microscope operated at an acceleration voltage of 80 kV.

Drying of suspensions

Different drying methods were applied to the suspensions just after mixing. Oven drying (OD) was performed at 105 °C for 24 h in glass beakers. Prior to freeze drying (FD), CNF suspensions (about 20 mL) were frozen in vials at a temperature of –80 °C for 24 h. Frozen suspensions were then transferred to a

Virtis Freezemobile 25 SL freeze dryer, which has a condenser temperature of –80 °C and a vacuum of 11 mTorr. Lyophilization was allowed to continue for 72 h. Supercritical drying (SCD) of the prepared suspension was conducted on the Tousimis Samdri PVT-3 Critical-Point dryer. Four steps were involved in this process: (1) dehydration of aqueous suspension with a series of ethanol solutions (50, 75, 95, and 100%) was performed before drying until water was completely replaced with ethanol, (2) replacement of ethanol with liquid CO₂, and (3) liquid CO₂ and the cellulose mixture is pressurized and heated to the supercritical conditions, and (4) the liquid CO₂ is eliminated by decompression to the atmosphere. A novel spray-drying method was conducted using a Mini Spray Dryer B-290 (Buchi, Switzerland). Details of the spray drying process are the subject of a provisional patent application.

Scanning electron microscopy (SEM)

SEM studies on the morphologies of dried samples were carried out using an AMR 1000 (AMRay Co.) scanning electron microscope. All samples were sputter-coated with gold before the microscopic observations were obtained. SEM images were taken at an accelerating voltage of 10 kV at various magnifications.

Particle size analysis

Quantitative characterization of particle size distribution was conducted using a Morphologi G3S system (Malvern, UK). The Morphologi G3S system provides the ability to measure the morphological characteristics (size and shape) of particles. The principle of the operation is based on digital image analysis utilizing an optical microscope. A sample is prepared and placed on the measurement slide or plate. Then the sample is scanned with transmitted or reflected light and high-resolution digital images are produced. Using the optical microscope under this situation, a two dimensional (2D) projected image of the three dimensional (3D) particles are obtained. The captured high-resolution image is then analyzed with the integrated analysis software to obtain the particle size characteristics. The area of captured 2D image for each particle is converted to a circle of same area and the diameter of the circle is reported as the circle

equivalent (CE) diameter of the particle. During the 2D image capturing process, a technique called Z stacking can be used to better characterize the 3D particles. A 3D particle sitting on the measurement plate cannot be completely in contact with the bottom plate surface. Since the objective lens of the instrument exhibits a narrow depth of field under high magnification, accurate focus cannot always be achieved across the entire body of a 3D particle. Z stacking is a utility that takes several images of the sample, each at different Z heights (Z axis is the direction normal to the measurement plate) and then overlays to form a single composite image. In this study, identical volumes of CNC and NFC powders (5 mm^3) were uniformly dispersed onto a glass plate using an integrated sample dispersion unit (SDU) with a dispersing pressure 0.5 MPa, injection time 10 ms, and settling time 60 s. The powder sample is first placed in a holder of SDU and held by $25 \text{ }\mu\text{m}$ carrier foils. Another carrier foil is placed in the top of the holder. Air pressure is then applied to break the foil and the resulting turbulence disperses the samples onto the measurement glass plate uniformly. After dispersion, a suitable objective lens was chosen according to the particle sizes. In this work, an objective lens of $50\times$ which corresponds to 2,468 times magnification was selected to take the 2D image of the three dimensional (3D) particles. Z stacking with additional two layers above initial focus was used to take three images of the sample, each at different Z heights (0, 3.6, and $7.3 \text{ }\mu\text{m}$) and then overlays to form a single composite image. Image analysis converted the captured image for each particle to a circle of same area and the circle equivalent (CE) diameter distribution of the characterized particles were reported as the particle size distribution.

Results and discussion

Characterization of cellulose nanofibrils in suspension

The prepared NFC and CNC suspensions at 2 wt. % are shown in Fig. 1a. The NFC suspension is milky white while the CNC suspension is a bluish translucent solution. Quantitative characterization of cellulose nanofibril size distributions in suspensions was performed on a 0.1 wt. % suspension using dynamic light

scattering (DLS). The obtained hydrodynamic diameter distributions of NFC and CNC at 0.1 wt. % are shown in Fig. 1b by intensity. A single peak at around 1,000 nm (from 712 to 1,484 nm) was observed on the NFC size distribution curve while two peaks at around of 35 (from 24 to 44 nm) and 165 nm (from 91 to 295 nm) were on the CNC curve (Table 1). Based on the Mie theory (Mie 1908), size distributions can be converted into volume distribution as shown in Fig. 1c. The size distribution by volume is slightly different than the measured size distribution by intensity. For CNC, a volume of about 76% is in the particle size range of 21–51 nm while about 24% are in the size range of 79–342 nm. The dimensions of NFC and CNC in suspension were also examined directly using a transmission electron microscope and the obtained micrographs of NFC and CNC are shown in Fig. 1d, i. Both NFC and CNC showed needlelike fibrils (Fig. 1d, g). NFC showed greater dimensions (diameter and length) than those of CNC, as indicated by the DLS measurement. A portion of relatively short and large cell wall sections (chunks) in the NFC suspension were also observed (Fig. 1e, f). A large aggregation of many individual fibrils was also observed in Fig. 1f. At the same time, entanglement of NFC (Fig. 1e) and CNC (Fig. 1h, i) fibrils occurred when air dried at a concentration of 0.001 wt. %.

Oven drying of cellulose nanofibril suspensions

Oven drying (OD) was conducted by exposing the suspensions in a conventional laboratory oven at $105 \text{ }^\circ\text{C}$ with circulating air. The schematic of the drying process is shown in Fig. 2a. Water evaporation can be divided into three parts (Brinker and Scherer 1990; Scherer 1990; Mujumdar and Devahastin 2000): (1) the constant rate-drying period, (2) the first falling rate-drying period, and (3) the second falling rate-drying period. In the constant rate drying period, CNFs move together with the shrinkage of suspension volume as water evaporates. In this process, the capillary forces which are mainly used to move cellulose nanofibrils increases as a function of water evaporation. When the cellulose nanofibril surface or partial surfaces are exposed, the first falling rate-drying period begins and water evaporation primarily takes place over the cellulose nanofibril surfaces. The capillary tension reaches a maximum value and vapor diffusion begins to take over. Simultaneously,

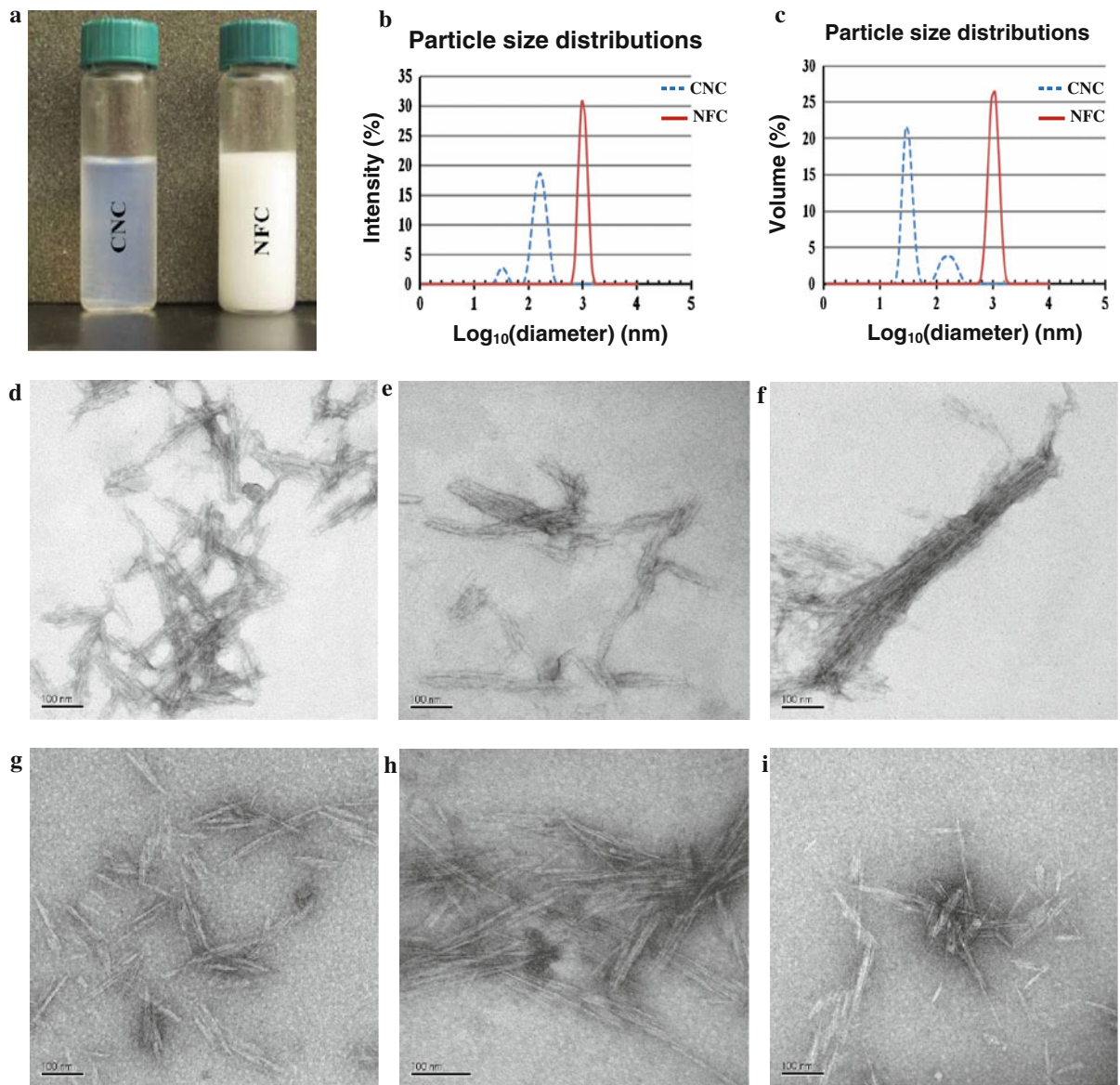


Fig. 1 Characterization of cellulose nanofibrils in suspension. **a** Cellulose nanocrystal (CNC) and nanofibrillated cellulose (NFC) suspensions. **b** Size distribution of NFC and CNC by intensity. **c** Size distribution of NFC and CNC by volume.

d–f Transmission electron microscopy (TEM) micrographs of negatively stained NFC. **g–i** TEM micrographs of negatively stained CNC

the cellulose nanofibrils move closer together. When the rate of transferring water from the interior of the cellulose nanofibril suspension to the exposed surface is smaller than the water diffusion rate on the surface, drying enters the second falling rate-drying period and completely occurs inside the cellulose nanofibril suspension. At this moment, the distance between the cellulose nanofibrils or nanocrystals becomes

much smaller and the molecular contact is finally attained because of the combined effect of capillary and diffusion forces. Under this situation, strong intermolecular hydrogen bonds develop to form a continuous fiber network and a relatively solid bulk material. Morphologies of the resulting CNC and NFC are shown in Fig. 2. The two suspensions formed bulk materials with different surface roughness and fracture

Table 1 Comparison among different CNF drying methods

Drying method	Particle size in suspension		Dried particle size		Morphology	Advantages	Disadvantages
	CNC (nm)	NFC (nm)	CNC	NFC			
Oven drying	24–44	712–1,484	Hundreds of microns to millimeters depends on drying process		Bulk network structure	Well established industrial processes, e. g. paper industry	Forms bulk material and loses the nano-scale dimensions of CNF
Freeze drying	91–295		Nano-scale in thickness and microns to millimeters in width or length		Ribbon-like structure	Maintain one dimension in nano-scale and well established process	Agglomeration of CNF and high cost
Supercritical drying			Nano-scale fibrous NFC		Fibrous and network	Maintaining nano-scale dimensions of the CNF	Complicated process using solvent replacement, high cost and impractical scale up.
Spray-drying			D [n, 0.9] = 6.76 μm	D [n, 0.9] = 7.48 μm	NFC: irregular fibril structure CNC: spherical particles	Low cost and scalable continuous drying process, controllable particle size	Some agglomeration, the particle sizes range from nano to micron size.

morphology. Oven-dried NFC exhibits a smoother top surface (Fig. 2b) than the bottom surface (Fig. 2c). Long time settling of the prepared NFC suspensions at room temperature precipitated the large particles to the bottom, indicating that the NFC suspension is not thermally stable. Parts of the fibers in the original suspension were short in length and large in diameter (Fig. 2c, d) which is consistent with the observations in Fig. 1e, f. The surfaces of dried CNC were much smoother than those of NFC, indicating a denser packing for CNC. This may be attributed to the much smaller size of cellulose nanocrystals in the suspensions compared with that of NFC.

Freeze drying of cellulose nanofibril suspensions

Freeze drying (FD) is a two-step operation: (1) freezing by refrigeration, and (2) drying under reduced pressure by sublimation of the frozen water and by desorption of water that did not freeze. Accordingly, three stages are involved in freeze drying: (1) freezing stage, (2) primary drying stage, and (3) secondary drying stage. The freezing stage is the first step to separate CNFs from water (free water and freezing bound water) which is in the form of ice crystals. The primary drying stage is used to sublime the separated ice crystals formed in the first stage while the nonfreezing bound water absorbed by CNFs is mainly removed during the secondary drying stage. The overall freeze drying process depends significantly on the freezing stage (Liapis et al. 1996; Bruttini et al. 2001) and CNF agglomeration may occur during the third stage. In the third stage, the nonfreezing bound water is removed by heating the product under vacuum. The water vapor thus diffuses and may induce structural changes and displacement of CNFs. The morphologies of freeze-dried NFC and CNC are shown in Fig. 3. The dried samples from the two suspensions formed similar plate-like materials with different sizes (Fig. 3a, d), differing from oven-dried CNF. The large length (several hundred micrometers) and width (tens to hundreds of micrometers) are the result of the lateral agglomeration of cellulose nanofibrils. This lateral fibril aggregation has also been demonstrated by Hult et al. (2001). The thickness of these plate-like materials can reach nanometer size. A close-up evaluation of the surface morphologies shows that the FD samples (Fig. 3c, f) are similar to those that were oven dried (Fig. 2d, g). The

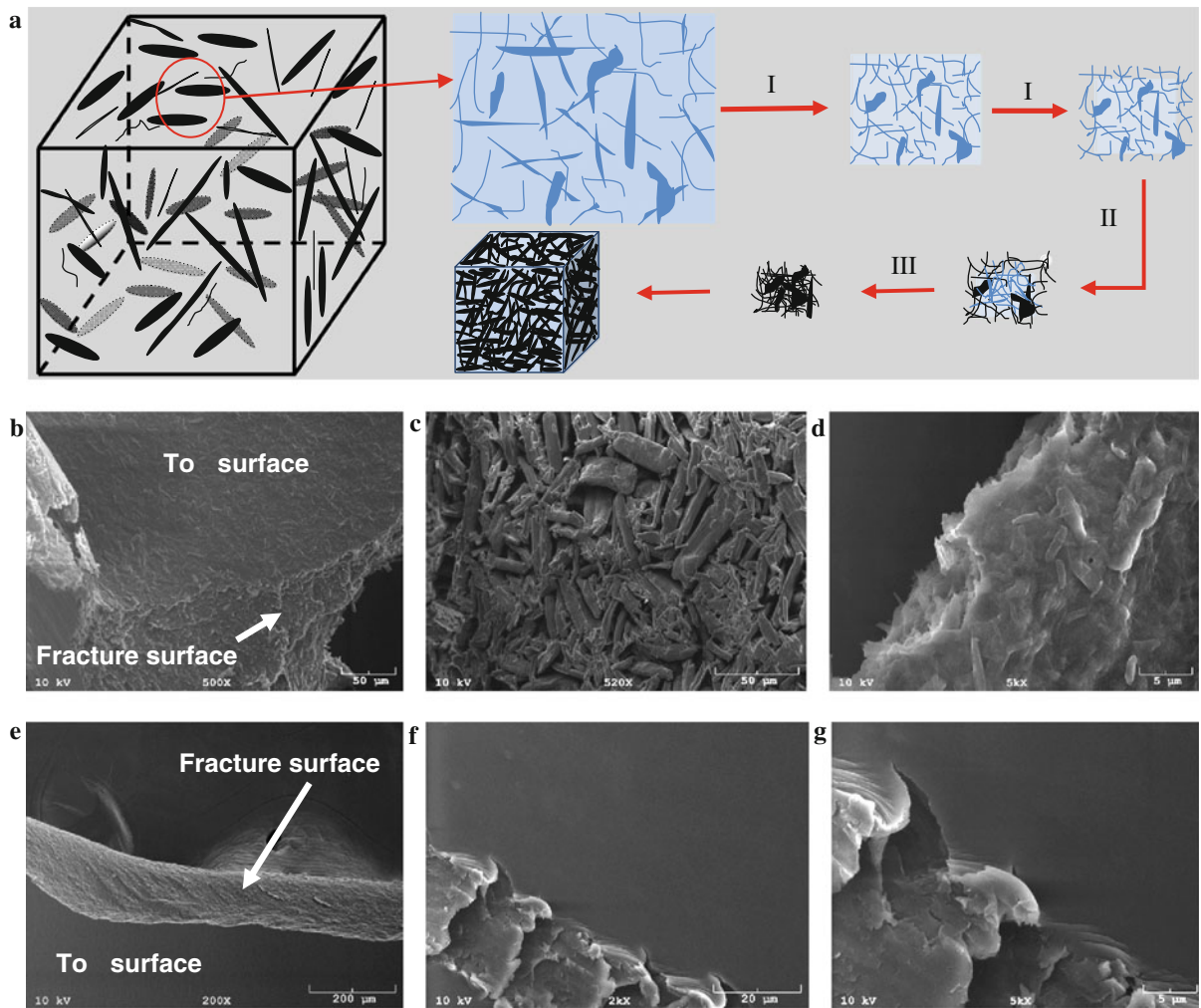


Fig. 2 Oven drying of cellulose nanofibril suspensions. **a** Schematic of the oven drying process for cellulose nanofibril suspensions. **b–d** Morphologies of oven-dried nanofibrillated cellulose (NFC). **e–g** Morphologies of oven-dried cellulose nanocrystals (CNC)

characterization of freeze-dried material is also summarized in Table 1. During the freeze drying process, the capillary forces are minimized (Pelton 1993) and no bulk material is formed. Therefore, capillary forces are mainly responsible for the formation of bulk material in the oven drying processes. The lateral aggregation may be driven by diffusion forces or perhaps by hydrogen bonding. This may further indicate that the cellulose nanofibrils in the suspension simply align laterally with many layers. Each layer has different amounts of nanofibrils laterally bonded. Elazzouzi-Hafraoui et al. (2008) demonstrated that CNC consisting of several laterally parallel crystallites has the dimensions of a nanofibril. Derived from the sheet structure of cellulose, the proposed weak

hydrogen bonds (Nishiyama et al. 2003) or hydrophobic bonds (Jarvis 2003) between different sheets of cellulose fibrils are more easily broken than are lateral hydrogen bonds (Klemm et al. 1998).

Supercritical drying of cellulose nanofibril suspensions

The morphologies of supercritical dried samples from NFC suspensions are shown in Fig. 3g–i. Using the process of supercritical drying (SCD), capillary pressure among the vapor–liquid interfaces and the solid cellulose nanofibrils is excluded (Wang et al. 2007). As the liquid CO_2 is removed, separated cellulose fibrils or a linked cellulose network remains.

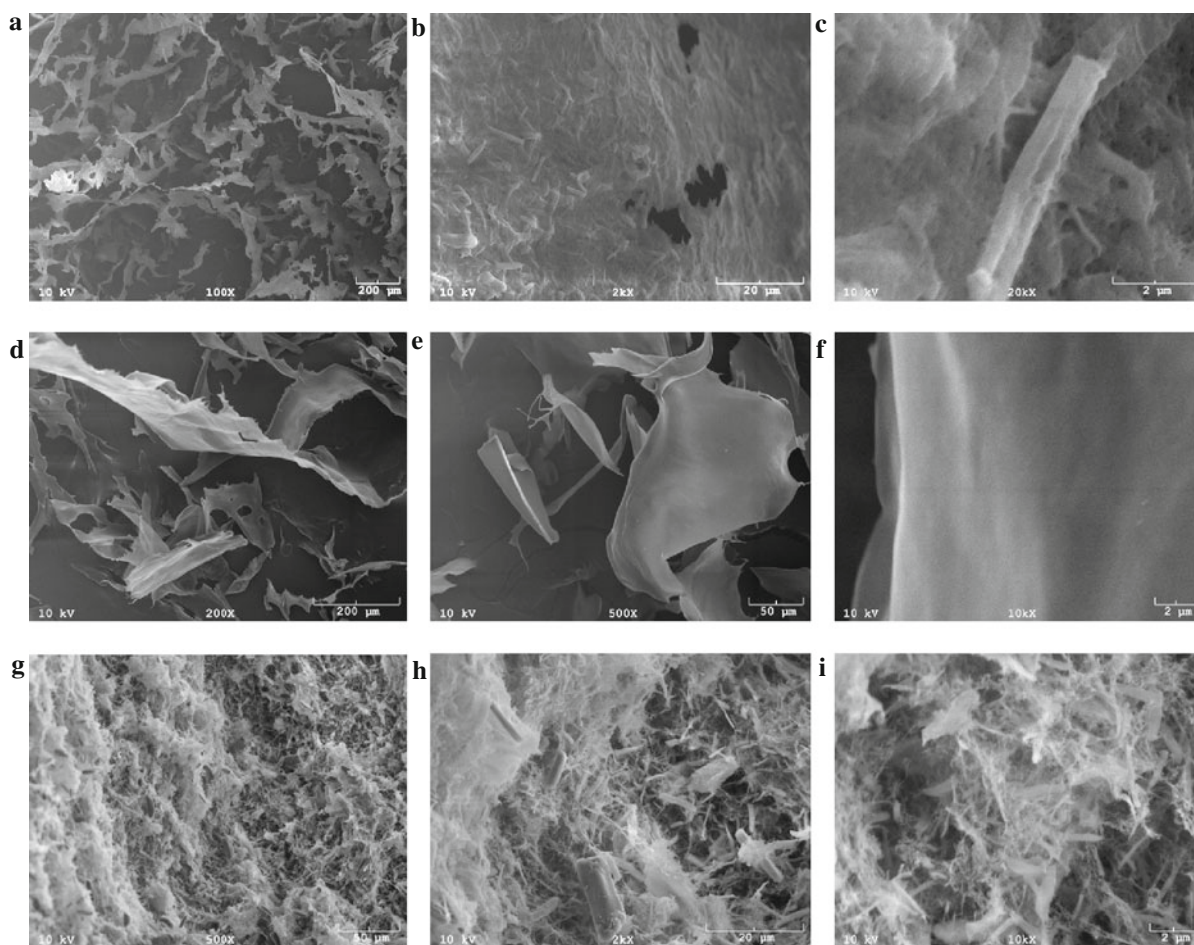


Fig. 3 Morphologies of freeze dried and supercritical dried cellulose nanofibrils. **a–c** Morphologies of freeze dried nanofibrillated cellulose (NFC). **d–f** Morphologies of freeze dried cellulose nanocrystal (CNC). **g–i** Morphologies of supercritical dried NFC

During the attempted dehydration of the CNC suspensions, complete replacement of the water in the suspension by using ethanol was not possible. Therefore, SCD was not applied to the CNC suspensions and no dry form of CNC was obtained. A possible reason for the poor ethanol dehydration in the CNC suspension might be attributed to the strong three-dimensional hydrogen bonding formed among the water molecules and cellulose nanocrystals. As seen in the micrographs of Fig. 3g–i, nano-scale cellulose fibrils with the diameter of about 100–200 nm were observed. Replacement of water with liquid CO₂ in SCD can reduce the lateral agglomeration of CNFs. However, cellulose nanofibril aggregates were also observed during ethanol dehydration using the SCD method (Thimm et al. 2000). This can also be

demonstrated by comparing fibril dimensions in Fig. 3 with those in the TEM micrographs of Fig. 1. The nanofibril size in the original suspensions is smaller than those shown in the micrographs. These micrographs have also demonstrated that large diameter and short length fibrils existed in the NFC suspension which is consistent with the TEM micrographs. In addition, entanglement of fine fibrils was also observed in Fig. 3g–i.

Spray-drying of cellulose nanofibril suspensions

Spray drying (SD) is a well-established technique that has been used in many areas, including the food, pharmaceutical, ceramic, polymer, and chemical industries. The critical cost analyses of the spray-drying

process have encouraged the acceptance of spray-drying as a standard industrial dehydration method (Hardy 1955; Quinn 1965). One of the major concerns about the inefficiency of the spray-drying process (low solid contents requirements) has also been eliminated (Quinn 1965). The relatively low labor and maintenance costs demonstrate that spray-drying can be used for those applications where specific product characteristics are required. Drying of CNF suspensions in a spray dryer (B-290) was accomplished through atomization in contact with hot air (Fig. 4a). A two-fluid atomization system was used. CNF suspensions were first pumped through a nozzle and formed the suspension film. The flowing hot gas was applied to mix the suspension externally. The momentum transfer between gas and suspension film disrupts the suspension film into ligaments (Dombrowski and Johns 1963) and then into droplets with diameters from several to tens of micrometers (Thybo and Hovgaard 2008). The droplets evaporate as they fall through the dryer chamber. Cyclone separation was used in the following to form the dry powder from moist air. Drying of droplets from the CNC suspension occurred in three steps similar to those which occurred with oven-dried samples. The mechanism for drying of CNC is shown in Number 2 of Fig. 4a. The morphologies of the spray-dried CNC samples are shown in Fig. 4b–d. Spherical particles were obtained. Concurrently, rough surfaces were observed for the spherical particles. This roughness was caused by the agglomeration of needle-shaped single CNC (Fig. 4d). For the NFC suspension, two different droplets may be formed during the atomization process: (1) NFC droplets with no NFC fibrils protruding and (2) droplets with partial NFC fibrils protruding. The length of the original fibrils in the suspension drives the difference. Drying the first kind of NFC droplet forms small spherical particles configured much the same as with CNC. For the second kind of NFC droplet, a portion of the original long NFC fibrils protrudes outside the droplet. Here, there is no constant rate drying period. The corresponding drying mechanism is shown in Number 3 of Fig. 4a. Agglomerated NFC particles were formed by the attachment of small NFC fibrils in the suspension to longer NFC fibrils. Irregular shaped particles were obtained. For both NFC and CNC samples, particles with the size of several microns were observed in the SEM micrographs. At the same time, a portion of the

particles with nano-scale dimensions (hundreds of nanometers) was also observed. Quantitative characterization of the particle size distributions with more than 200,000 particles of CNC and NFC was measured using a morphological analyzer. The frequency curves of circle equivalent (CE) diameter distribution of CNC and NFC particles are shown in Fig. 5a. The standard percentile readings $D(n, 0.1)$, $D(n, 0.5)$, and $D(n, 0.9)$ of CE diameter derived from the statistics of the distribution are also shown in Fig. 5b. The CE diameters of CNC at 10, 50, and 90 percentile are 1.31, 3.06, and 6.76 μm while the distribution for NFC samples is 1.59, 2.96, and 7.48 μm . It can be seen from the frequency curves in Fig. 5a that a small portion of the particles (NFC and CNC) are in the nano-scale dimension (CE diameter is smaller than 1 μm). It needs to be pointed out that the particle size under about 0.2 μm cannot be identified accurately by the Morphologi G3S equipment. This is caused by the limit of resolution of the optical microscope. It is envisioned that the spray-drying process can be further manipulated to control the droplet sizes. Spray-drying studies are currently ongoing.

Different drying techniques for various CNF suspensions provide cellulose products with different sizes and morphologies (Table 1). The advantages and disadvantages of the four different methods are also discussed in Table 1. Drying CNF suspensions in an oven cannot be used to produce nano-scale cellulose fibrils. Drying of CNF suspensions using FD, SCD, and SD can produce powdery products having nano-scale dimensions. From the point view of obtaining nano-scale cellulose fibrils, SCD appears to be the best technique to preserve the nano-dimensions of CNF, as demonstrated by the TEM and SEM micrographs. However, the method of SCD is appropriate for drying small amounts of nanofibrils and may be too expensive to perform on an industrial scale (Pakowski 2007). At the same time, the produced nanofibrils using SCD are easily entangled to form solid aggregates. Freeze drying provides a ribbon-like material assumed to be the product of a significant lateral aggregation. Spray-drying forms particles with different morphologies which are dependent on the sources of CNFs. Fifty percent of dried CNC and NFC particles are below 3.06 and 2.96 μm in CE diameter and 90% are below 6.76 and 7.48 μm . A small portion of the spray-dried particles are observed in the nano-scale range (several hundred nanometers).

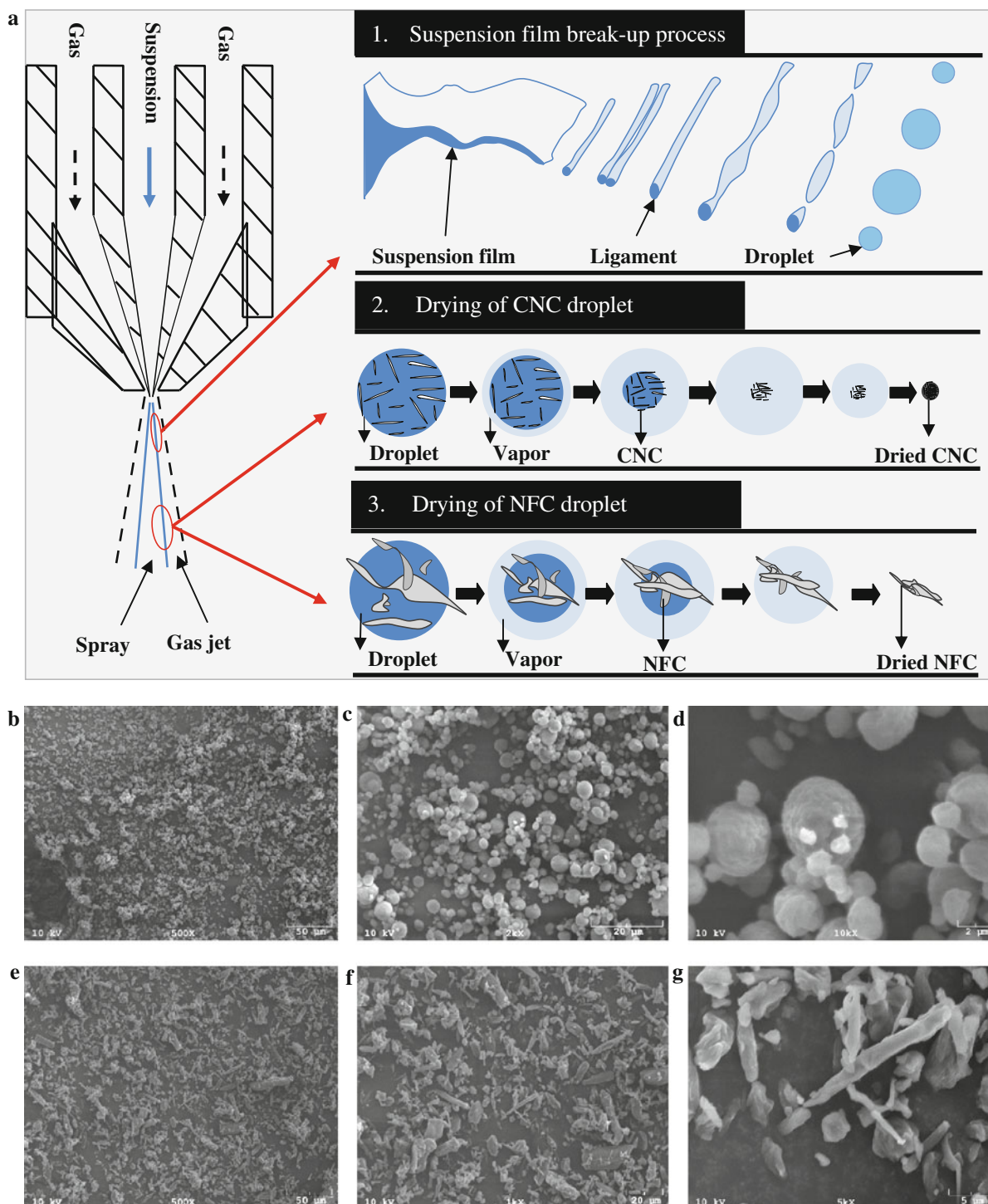


Fig. 4 Spray-drying of cellulose nanofibril suspensions. **a** Mechanism of spray-drying process. **b–d** Morphologies of spray-dried cellulose nanocrystal (CNC). **e–g** Morphologies of spray-dried nanofibrillated cellulose (NFC)

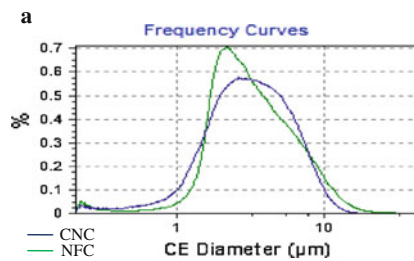


Fig. 5 Particle size distribution of spray-dried cellulose nanofibrils. **a** Frequency curves of number based circle equivalent diameter (CE) of nanofibrillated cellulose (NFC)

In term of process economics, as reported by the food industry (Filkova et al. 2007) or the flavor industry (Desobry et al. 1997), freeze drying is 5–10 times more expensive than spray-drying. In addition, involving solvent exchange in the process of supercritical drying complicates the drying process and makes this process expensive (Pakowski 2007). Based on the results obtained by examining the various lab scale drying methods, spray-drying is proposed to be a suitable manufacturing process which can be used to dry cellulose nanofibril suspensions.

Conclusions

The morphological properties of the dried cellulose nanofibrils are dependent on the particular drying method and the starting materials (NFC and CNC). The agglomeration mechanisms occurring among the cellulose nanofibrils are different for each drying method. SCD and FD created highly networked structures of cellulose agglomerates with multi-scalar dimensions including the nano-scale. An agglomeration mechanism was introduced for the SD method, showing how the dried particulates could be formed. Only the SD method produced particulates of dried cellulose which, range in size from nano to micron, and are viewed as potentially suitable for use as additives or fillers in composite manufacturing utilizing conventional thermoplastic compounding techniques. The highly-networked structures of dried cellulose from SCD and FD may limit the use of the products in particular composite applications since the difficulties in dispersion would remain as a barrier in conventional thermoplastic compounding. In terms of nano material production from cellulose suspensions,

b

Sample	CE diameter (μm)		
	D(n,0.1)	D (n, 0.5)	D (n, 0.9)
CNC	1.31	3.06	6.76
NFC	1.59	2.96	7.48

and cellulose nanocrystal (CNC). **b** The standard percentile readings of CE diameter distribution of NFC and CNC in **a**

SD is suggested for its potential capability to create particulates on the nano-scale.

Acknowledgments The authors acknowledge the US Army Corps of Engineers, Engineering R&D Center, and the Maine Agricultural and Forestry Experiment Station McIntire-Stennis Project ME09615-06 for financial support. The content and information does not necessarily reflect the position of the funding agencies. Maine Agricultural and Forest Experiment Station Publication Number 3242.

References

- Beecher JF (2007) Organic materials: wood, trees and nanotechnology. *Nat Nanotechnol* 2:466–467
- Bloch J (2011) UMaine to build nation's only cellulose nanofibrils pilot plant. [http://umaine.edu/news/blog/2011/10/28/umaine-to-build-nation's-only-cellulose-nanofibrils-pilot-plant/](http://umaine.edu/news/blog/2011/10/28/umaine-to-build-nation-s-only-cellulose-nanofibrils-pilot-plant/)
- Brinker CJ, Scherer GW (1990) Drying. In: Brinker CJ, Scherer GW (eds) *Sol-gel science: the physics and chemistry of sol-gel processing*, 1st edn. Academic Press Limited, London, pp 453–513
- Bruttini R, Grosser OK, Liapis AI (2001) Energy analysis for the freezing stage of the freeze drying process. *Dry Technol* 19:2303–2314
- Clark JD'A (1985) Fibrillation and fiber bonding. In: Clark JD'A (ed) *Pulp technology and treatment for paper*, 2nd edn. Miller Freeman Publications, San Francisco, pp 160–180
- Desobry SA, Netto FM, Labuza TP (1997) Comparison of spray-drying, drum-drying and freeze-drying for β -Carotene encapsulation and preservation. *J Food Sci* 62: 1158–1162
- Dombrowski N, Johns WR (1963) The aerodynamic instability and disintegration of viscous liquid sheets. *Chem Eng Sci* 18:203–214
- Eichhorn SJ, Dufresne A, Aranguren M, Marcovich NE, Capadona JR, Rowan SJ, Weder C, Thielemans W, Roman M, Renneckar S, Gindl W, Veigel S, Keckes J, Yano H, Abe K, Nogi M, Nakagaito AN, Mangalam A, Simonsen J, Benight AS, Bismarck A, Berglund LA, Peijs T (2010) Review:

- current international research into cellulose nanofibres and nanocomposites. *J Mater Sci* 45:1–33
- Elazzouzi-Hafraoui S, Nishiyama Y, Putanus J, Heux L, Debreuil F, Rochas C (2008) The shape and size distribution of crystalline nanoparticles prepared by acid hydrolysis of native cellulose. *Biomacromolecules* 9:57–65
- Filkova I, Huang LX, Mujumdar AS (2007) Industrial spray drying systems. In: Mujumdar AS (ed) *Handbook of industrial drying*, 3rd edn. CRC Press, New York, pp 215–254
- Gardner DJ, Oporto GS, Mills R, Samir MASA (2008) Adhesion and surface issues in cellulose and nanocellulose. *J Adhes Sci Technol* 22:545–567
- Habibi Y, Lucia LA, Rojas OJ (2010) Cellulose nanocrystals: chemistry, self-assembly, and applications. *Chem Rev* 110:3479–3500
- Hardy WL (1955) Costs process and construction-spray drying cost analysis shows labor is largest item, utilizes constant. *Ind Eng Chem* 47:73A–74A
- Herrick FW, Casebier RL, Hamilton JK, Sandberg KR (1983) Microfibrillated cellulose: morphology and accessibility. *J Appl Polym Sci Appl Polym Symp* 37:797–813
- Hiemenz PC, Rajagopalan R (1997) *Principles of colloid and surface science*. CRC Press, New York
- Hubbe MA, Rojas OJ, Lucia LA, Sain M (2008) Cellulosic nanocomposites: a review. *BioResources* 3(3):929–980
- Hult EL, Larsson PT, Iversen T (2001) Cellulose fibrils aggregation—an inherent property of kraft pulps. *Polymer* 42:3309–3314
- Hunter RJ (2001) *Foundations of colloid science*. Oxford Univ. Press, Oxford
- Jarvis M (2003) Cellulose stacks up. *Nature* 426:611–612
- Jeronimidis G (1980) Wood, one of nature's challenging composites. *Symp Soc Exp Biol* 34:169–182
- Klemm D, Philipp B, Heinze T, Heinze U, Wagenknecht W (1998) *Comprehensive cellulose chemistry*. Volume 1, fundamentals and analytical methods. Wiley-VCH, New York
- Klemm D, Kramer F, Moritz S, Lindstrom T, Ankerfors M, Gray D, Dorris A (2011) Nanocelluloses: a new family of nature-based materials. *Angew Chem Int Ed* 50:5438–5466
- Lawson CL, Hanson RJ (1995) *Solving least squares problems*. Society for industrial and applied mathematics (SIAM), Philadelphia
- Liapis AI, Pikal MJ, Bruttini R (1996) Research and development needs and opportunities in freeze-drying. *Dry Technol* 14:1265–1300
- Lindstrom T, Wagberg L, Larsson T (2005) On the nature of joint strength in paper—a review of dry and wet strength resins used in paper manufacturing. In: *Proceedings of 13th fundamental research symposium*, Cambridge, Pira International, Leatherhead
- Lyne LM, Galay W (1954) Studies in the fundamentals of wet web strength. *Tappi* 37(12):698–704
- McKenzie AW (1984) The structure and properties of paper. Part XXI: the diffusion theory of adhesion applied to interfiber bonding. *Appita* 37(7):580–583
- Mie G (1908) Beitrage zur optic truber medien, speziell kolloidaler metallosungen. *Ann Physik* 4:377–445
- Moon RJ, Marini A, Nairn J, Simonsen J, Youngblood J (2011) Cellulose nanomaterials review: structure, properties and nanocomposites. *Chem Soc Rev* 40:3941–3994
- Mujumdar AS, Devahastin S (2000) Fundamental principles of drying. In: Devahastin S (ed) *Mujumdar's practical guide to industrial drying*. Exergex Vorp, Montreal, pp 1–22
- Nakamura K, Hatakeyma T, Hatakeyma H (1981) Studies on bound water of cellulose by differential scanning calorimetry. *J Textile Inst* 72(9):607–613
- Nishiyama Y, Sugiyama J, Chanzy H, Langan P (2003) Crystal structure and hydrogen bonding system in cellulose I alpha from synchrotron X-ray and neutron fiber diffraction. *J Am Chem Soc* 125:14300–14306
- O'Connor B (2011) Ensuring the safety of manufactured nanocrystalline cellulose: a risk assessment under Canada's new substances notification regulations. <http://www.tappi.org/content/events/11nano/paper/11Nano03.pdf>. Accessed 21 June 2011
- Pakowski Z (2007) Modern methods of drying nanomaterials. *Transp Porous Med* 66:19–27
- Pelton R (1993) A model of the external surface of wood pulp fibers. *Nordic Pulp Paper Res J* 8(1):113–119
- Quinn JJ (1965) The economics of spray drying. *Ind Eng Chem* 57:35–37
- Scherer GW (1990) Theory of drying. *J Am Ceram Soc* 73:3–14
- Siqueira G, Bras J, Dufresne A (2010) Cellulosic bionanocomposites: a review of preparation, properties and applications. *Polymers* 2:728–765
- Siro I, Plackett D (2010) Microfibrillated cellulose and new nanocomposite materials: a review. *Cellulose* 17:459–494
- Thimm JC, Burritt DJ, Ducker WA, Melton LD (2000) Celery (*Apium graveolens* L.) parenchyma cell walls examined by atomic force microscopy: effect of dehydration on cellulose microfibrils. *Planta* 212:25–32
- Thybo P, Hovgaard L (2008) Droplet size measurements for spray dryer scale-up. *Pharm Dev Technol* 13:93–104
- Vartiaine J, Pohler T, Sirola K, Pylkkanen L, Alenius H, Hokkinen J, Tapper U, Lahtine P, Kapanen A, Putkisto K, Hiekkataipale P, Eronen P, Ruokolainen J, Laukkanen A (2011) Health and environmental safety aspects of friction grinding and spray drying of microfibrillated cellulose. *Cellulose* 18:775–786
- Wang B, Huang LX, Mujumdar AS (2007) Drying of nanosize products. In: Mujumdar AS (ed) *Handbook of industrial drying*, 3rd edn. CRC Press, New York, pp 713–727
- Weise U, Maloney T, Paulapuro H (1996) Quantification of water in different states of interaction with wood pulp fibres. *Cellulose* 3:189–202